Reactor Theory: Contributions of PHYSOR-2008 Conference

P. Ravetto

Politecnico di Torino,

Dipartimento di Energetica

Torino, Italy

General observation

- Large number of contributions presented to the Conference
- All chapters of classic and advanced reactor theory are addressed in the contributions
- Very hard to give an organic overview of the presentations

Nuclear data

- Data for actinides
- Delayed neutron data
- Anisotropy
- Adjustment
- Libraries, validation and application
- Covariance data (full session)
- Sensitivity analysis

Lattice calculations and group structure

- Double heterogeneity
- Cell calculation by the method of characteristics
- Ultrafine energy mesh and mesh refinement
- Adaptive energy mesh constructor for generation of multigroup libraries

Table 5

Percent relative error between APOLLO2 and TRIPOLI4's calculation using 1968 ECCO and 1499 AEMC meshes for 1D fast reactor cell.

Calculation	U238 Absorption		Pu239 Absorption	
	error	AME	error	AME
1968 ECCO	0,18%	0.22%	0,06%	0.21%
1499 AEMC	0,11%	0.36%	0,16%	0.26%

Table 6

Computational features of 1968 ECCO and 1499 AEMC meshes for 1D fast reactor cell.

Mesh	Storage memory space of the multigroup library	Selfshielding calculation time
1968 ECCO	0,60 Gb (100%)	827,1 s (100%)
1499 AEMC	0,236 Gb (39,3%)	476,3 s (57,6%)

Lattice calculations and group structure

- Double heterogeneity
- Cell calculation by the method of characteristics
- Ultrafine energy mesh and mesh refinement
- Adaptive energy mesh constructor for generation of multigroup libraries

Table 1
UO2 Benchmarks

Enr	HZP Eigenvalue		HFP Eigenvalue	
w/o	MCNP	PARAGON	MCNP	PARAGON
0.7	0.66587	0.66629	0.66085	0.66066
1.6	0.96089	0.96082	0.95244	0.95269
2.4	1.09828	1.09869	1.08980	1.08949
3.1	1.17655	1.17649	1.16708	1.16681
3.9	1.23894	1.23898	1.22943	1.22896
4.5	1.27466	1.27431	1.26445	1.26414
5.0	1.29842	1.29857	1.28864	1.28830

Table 2
MOX Benchmarks – Reactor Grade Pu

Enr	HZP Eigenvalue		HFP Eigenvalue	
w/o	MCNP	PARAGON	MCNP	PARAGON
1.0	0.94383	0.94389	0.93442	0.93396
2.0	1.01978	1.02029	1.00872	1.00834
4.0	1.07476	1.07598	1.06306	1.06292
6.0	1.10349	1.10483	1.09188	1.09196
8.0	1.12696	1.12827	1.11545	1.11524

Codes

- Large number of contributions
- Improvements and new features of existing codes
- Code validation and benchmarks (full session)

Analytical methods

- Few contributions specific to reactor theory
- Solution to full multigroup multilayer diffusion problem

Analytical solution to the multigroup multilayer diffusion problem

and the general solution to the recurrence is

$$\phi_j = \left[1 - \rho_j \rho_n^{-1}\right] f_{pj} \, . \qquad (18)$$

4.2. Criticality condition

For criticality

$$f_{pj} \equiv 0$$

and Eq.(16) becomes

$$\rho_n \phi_1 = 0 \, .$$

Numerical methods

- Large number of contributions
  - Assessment of features of numerical techniques
    - Analysis of stability of finite-difference schemes for source-iteration acceleration
    - Convergence of rebalance methods
    - Error estimation of S_N nodal methods

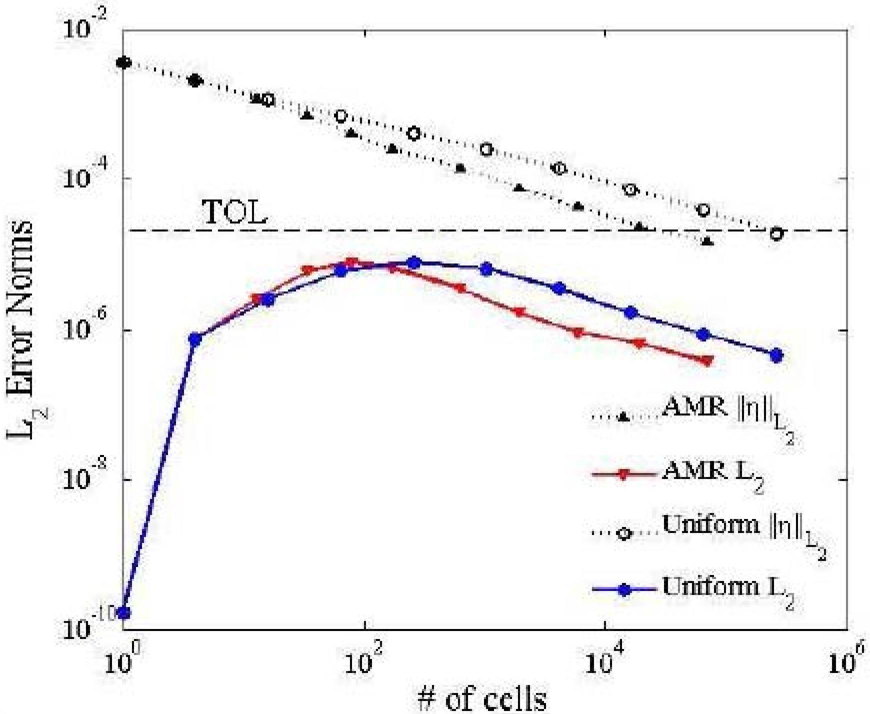

Fig. 2. L_2 error norms of the scalar flux for uniform (10 steps) and adaptive mesh (20 steps) refinements for the MMS problem. The global error estimator is shown to bound the L_2 error norm. AHOT-N $\Lambda = 0$.

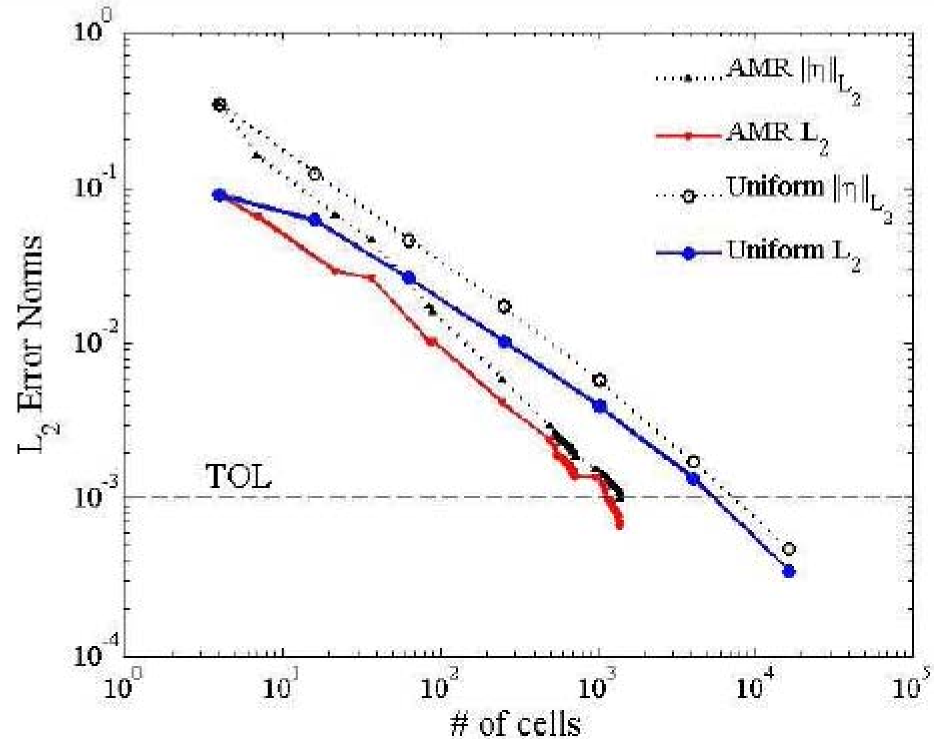

Fig. 3. L_2 error norms of the scalar flux for uniform and adaptive mesh (36 steps) refinements. The global error estimator is shown to bound the L_2 error norm. AHOT-N $\Lambda = 1$.

Numerical methods

– New applications of numerical methods
  - Laplace transform method extension to lattice calculation
  - Double P_N for cell-type calculations
  - Nodal methods for P_N

Numerical methods

– New methods

- Newton-Krylov discontinuous Galerkin method
- Krylov subspace method for eigenvalue calculation
- Scheme for higher-order mode calculation
- Discretization of unstructured geometry problems

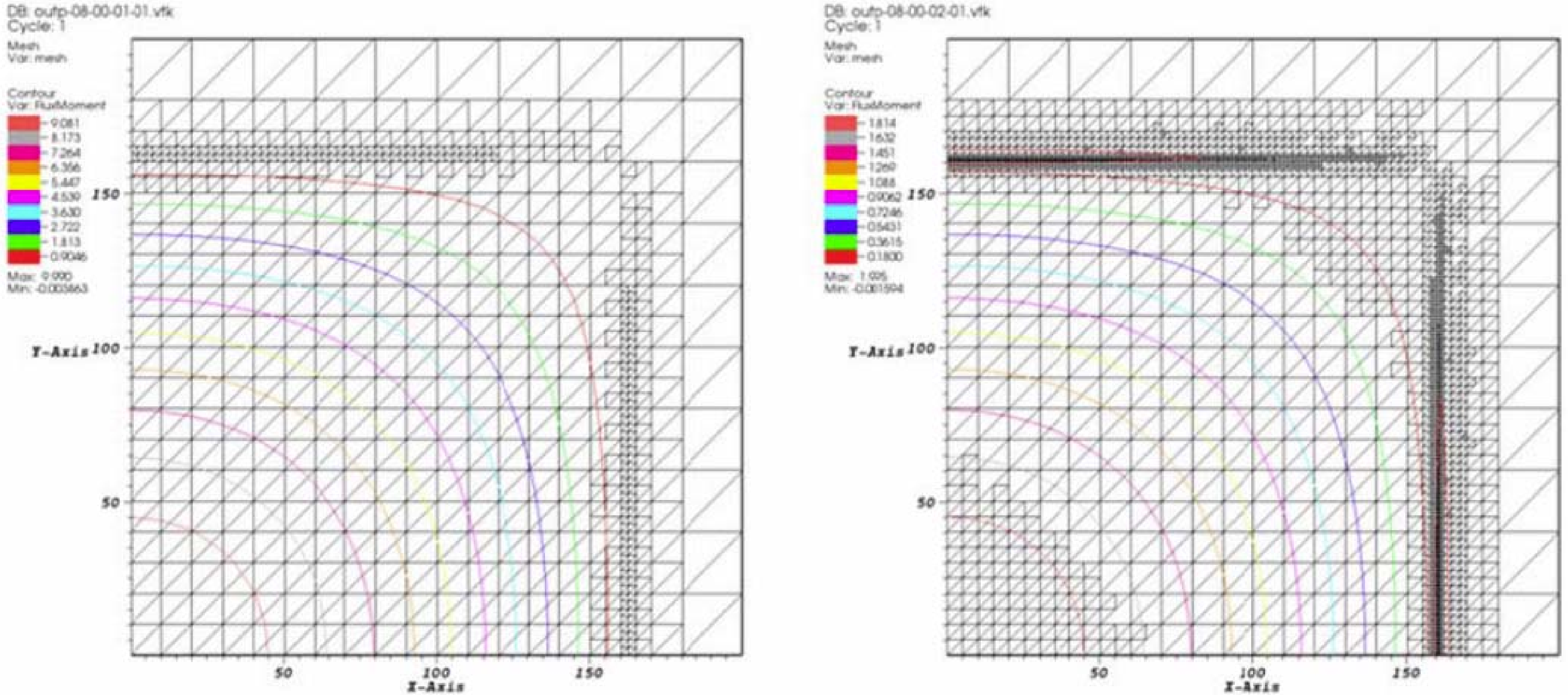

Fig. 6 Results (flux contour plots and adapted meshes) for the 2-g eigenproblem (left=fast flux; right=thermal flux).

Dynamics

- Quasi-static developments
- Acceleration of the numerical solution of reactor kinetic equations
- Time-dependent TORT

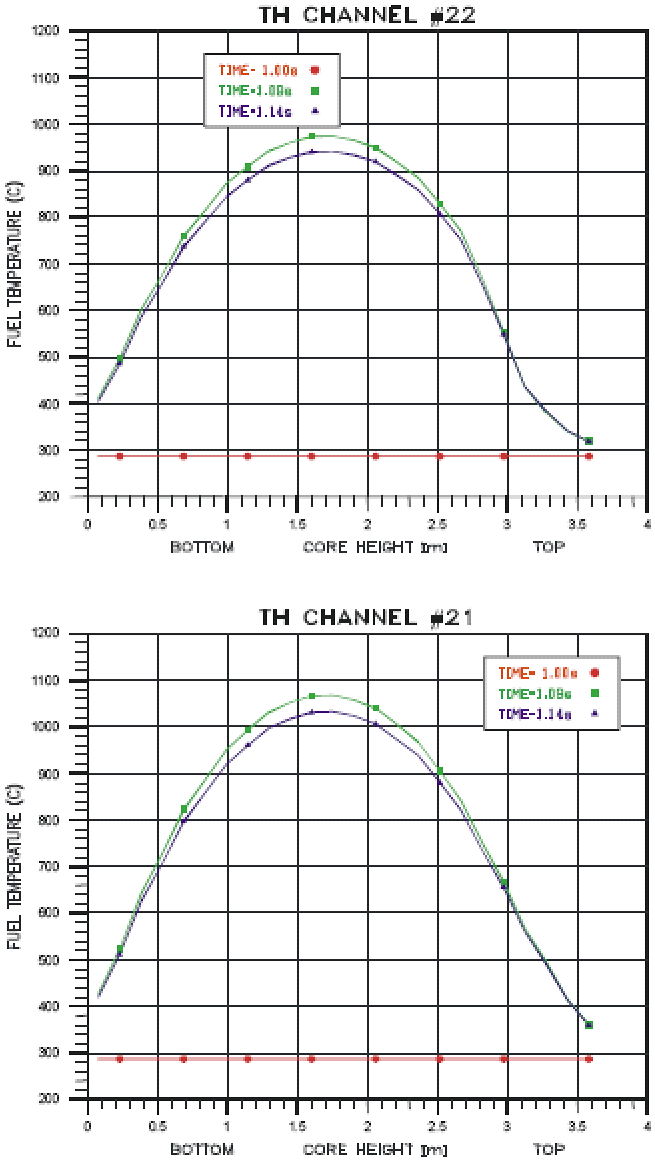

Fig. 10. Axial profiles of the radially averaged fuel temperatures in the E5 (top) and E4 (bottom) fuel assemblies at three different time steps.

Monte Carlo

- Feasibility of dynamic simulations and basic aspects
- Analysis of the basic problem of variance generation in the MC process
- Space-time reactor kinetics, coupling MC with kinetic equations, and verification with S_N
- Coupling of MC with thermal feed-back calculation

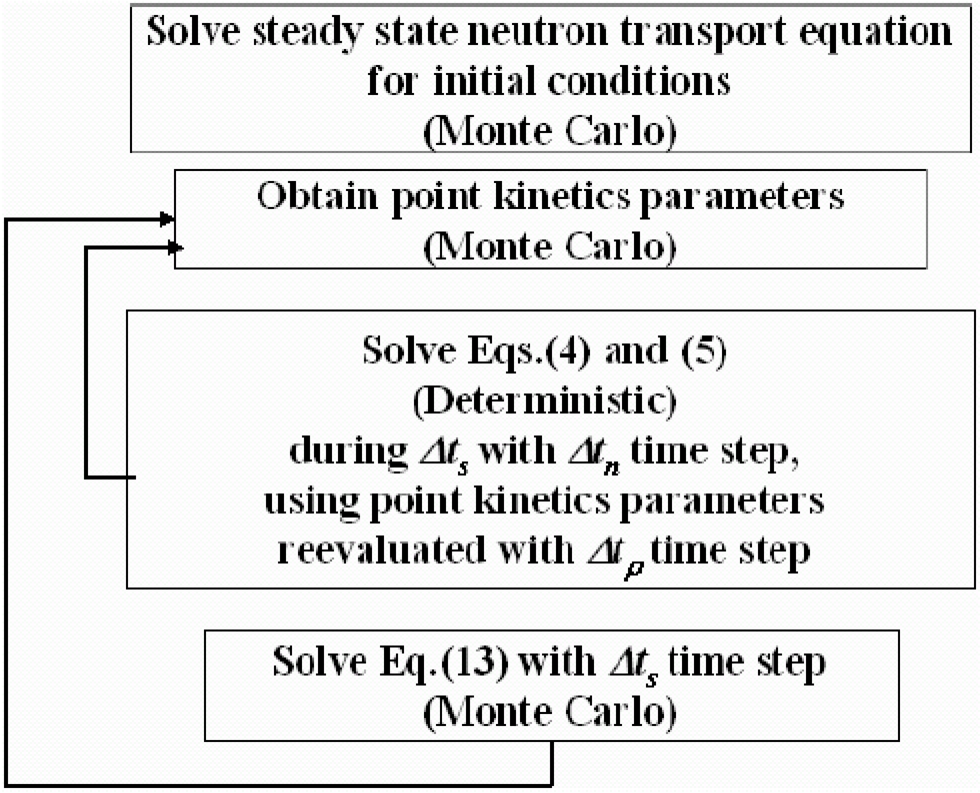

Fig. 1. Flow chart of Monte Carlo reactor kinetics method

Monte Carlo

- Feasibility of dynamic simulations and basic aspects
- Analysis of the basic problem of variance generation in the MC process
- Space-time reactor kinetics, coupling MC with kinetic equations, and verification with S_N
- Coupling of MC with thermal feed-back calculation

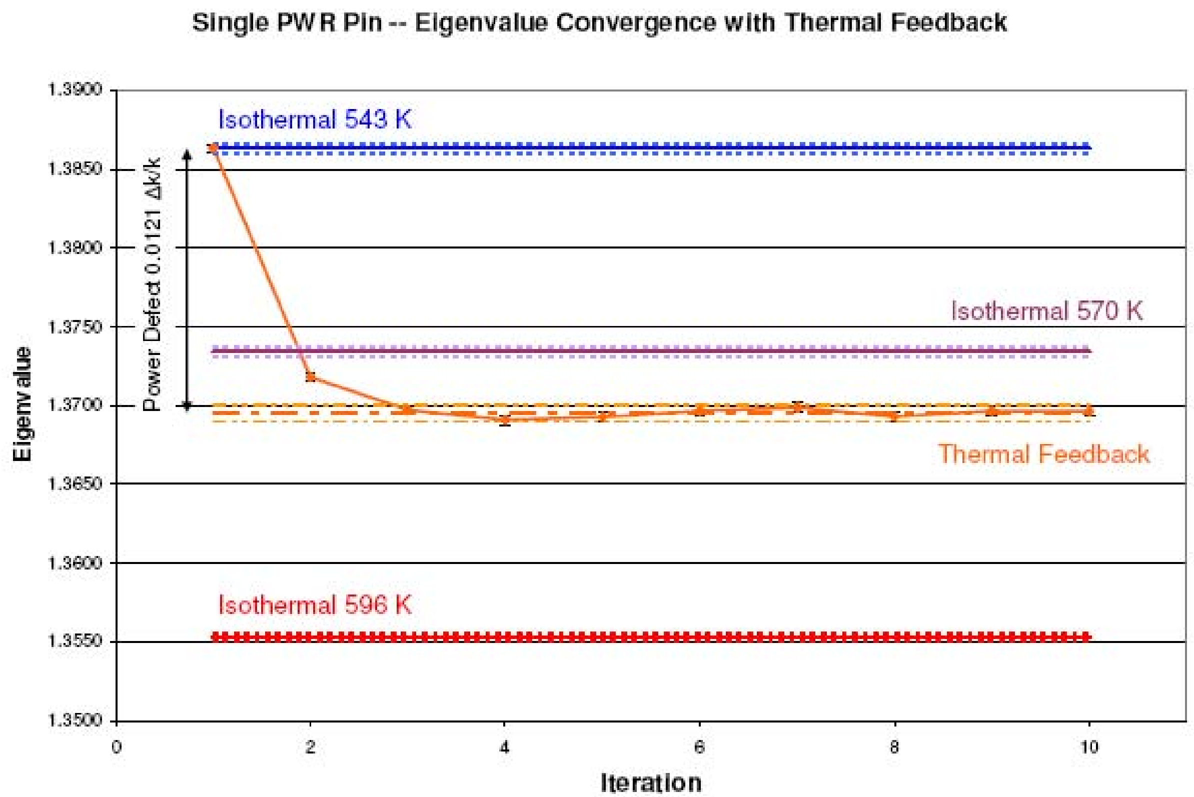

Temperature Defect (not shown) 0.0287 Δk/k

Fig. 1. Eigenvalue convergence with thermal feedback for single PWR fuel pin lattice. Thermal feedback convergence is shown relative to isothermal calculations with coolant temperatures at T_{inlet}, T_{outlet}, and T_{ave}. The 95% confidence intervals for each iteration are shown with error bars. The 95% confidence intervals for iteration-average values are shown by dashed lines.

Deterministic 3-D

- High-order diamond differencing scheme
- Local-global coupling

Table 1. Percent Error and Reference CPU Times Three-Dimensional MOX Fuel Assembly Problem with Fully Withdrawn Control Rods

	% Difference *k* Eigenvalue	% Ref CPU R Matrix Formulation	% Ref CPU Outer Iterations	% Ref CPU Total
I-P12-2	0.1206	1.11	0.11	1.22
I-P12-4	0.0305	1.15	0.84	1.99
I-P12-6	0.0092	1.18	5.26	6.44
I-P2	0.4346	0.10	0.13	0.23
I-P4	0.2114	0.19	1.17	1.36
I-P6	0.0906	0.29	7.77	8.06
I-P12	- -	1.90	98.1	100